Experimental assessment of the structural behavior of a masonry wall under horizontal cyclic loads

A. Costa, B. Silva, A. Costa, J. Guedes & A. Arêde
F.E.U.P. – Faculdade de Engenharia da Universidade do Porto, Porto, Portugal

ABSTRACT: This paper presents a numerical and experimental study on the cyclic behavior of a masonry wall from a house that collapsed during the July 9, 1998, earthquake in the Archipelago of Azores. It is divided into three parts: the first one contains the description, analysis, and interpretation of the outcome of the laboratory tests; the second one describes the wall's numerical model adopted for the simulation of the tests and presents the comparison with the experimental results; the last part concerns tests made on the wall after being reinforced.

Keywords: masonry, reinforcement, experimental testing, numerical modeling

1 LABORATORY TEST

1.1 *Brief description of the wall*

This work presents the experimental and numerical behavior of a wall from a house located at the parish of Pedro Miguel, Horta council, Faial Island (Fig. 1) in the Archipelago of Azores.

It is a traditional two-sleeve masonry wall filled with a poor material with low cohesion, typical of this Archipelago. On the outside, the wall is covered with mortar. The wall was transported by ship from its original location to the Laboratory for Seismic and Structural Engineering of the Faculty of Engineering of the Porto University (LESE - Laboratório de Engenharia Sísmica e Estrutural da FEUP) where it was set on a reinforced concrete block. The connection between the wall and the foundation was meant to be weak; a sand pillow was set between the two structures. A high rigid mixed structure of concrete and steel was set at the top of the wall to allow a uniform distribution of the horizontal and vertical loads applied during the test.

1.2 *Test methodology*

The test was carried out in the LESE to study the behavior of this masonry wall in terms of strength, ductility, and energy dissipation capacity under imposed cyclical horizontal displacements to simulate the effects of a horizontal seismic action.

Fig. 1. Building from where the wall was removed.

To reproduce the local conditions, two hydraulic jacks were set on the top of the wall against a reaction structure linked to the foundation through steel rods, to guarantee the existing vertical load. This system allowed a better distribution of the vertical load applied to the wall. The horizontal displacements were imposed using a hydraulic jack linked on one side to a reaction structure and, on the other, to the wall top through a hinged connection. The wall foundation was rigidly connected to the lab floor through high-strength prestressed rods (Fig. 2).

Fig. 2. Wall view and testing scheme.

The test was performed by a displacement control system that simultaneously collected data from all monitored spots: five load cells (one at each steel tie between the wall top reaction structure and the foundation, and one set on the actuator), and thirteen LVDTs; their location is illustrated in Figure 3. This figure also indicates the positive direction of the horizontal displacements. Spot 32 refers to the LVDT controlling the actuator.

2 ANALYSIS AND INTERPRETATION OF THE TEST OUTCOME

2.1 *Imposed displacements curve*

A set of horizontal displacements was imposed in the longitudinal direction (positive/negative) of the wall with peaks ranging from 0 to 10mm (Fig. 4). However, due to the different capacity of the actuator to respond to forward and backward movement, the displacements imposed in both directions were not the same.

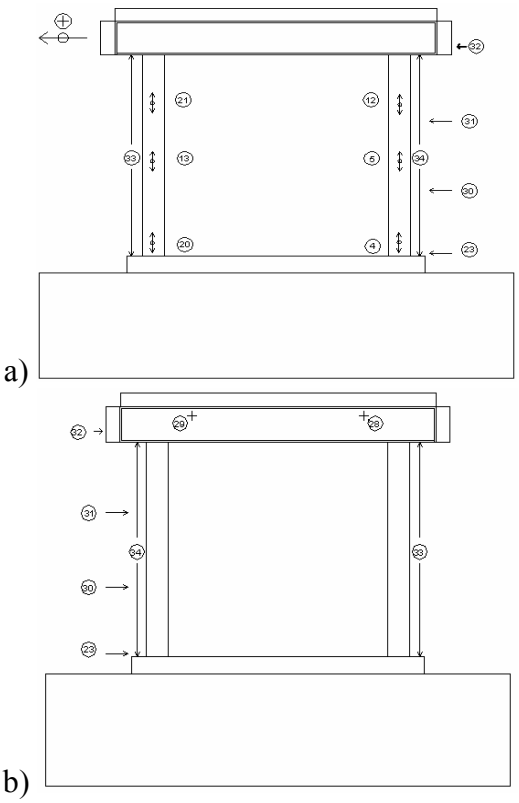

Fig. 3. LVDTs positioning: (a) front view, (b) back view.

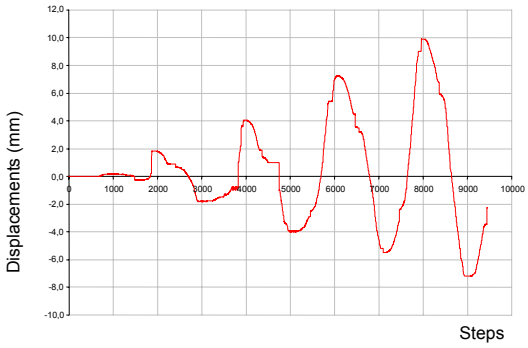

Fig. 4. Horizontal displacements series imposed on the top of the wall during the test.

2.2 *Analysis of the joints behavior*

The analysis of the behavior of the door columns joints cannot be performed separately; the behavior of one joint affects the others. Figures. 5 and 6 show the relationship between the wall's overall horizontal displacement at the application force spot 32 and the openings of the door columns joints at the right (4, 5, 12) and left (20, 13, 21) sides.

The next paragraphs analyze the results of these transducers.

2.3 *LVDT 4 and 20*

The outcome of these two LVDTs set near the basement was the expected. Along the horizontal displacements, the joints showed a consistent behavior: when one of the joints closed the other opened. In particular, when the displacement was imposed in the negative direction, the joint at spot 4 showed a closing tendency. However, when the wall moved in the positive direction, the observed decompression was not enough to open the joint. In general terms, this joint showed an overall displacement towards its closure. This behavior might be the result of an inside rearrangement of the joint particles, due to the vertical and tangential forces generated at the joint as a consequence of the applied forces. It is also noticed that the joint global displacement at this spot is quite small (~0.3mm towards closure), when compared to the other joints displacements at the same door column.

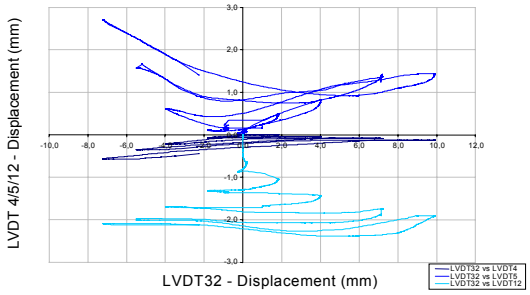

Fig. 5. Openings of the right side door column joints vs. the horizontal top displacements (LVDT 32).

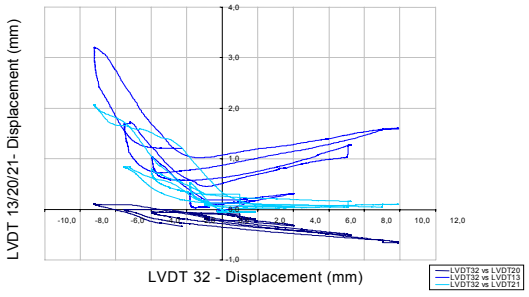

Fig. 6. Openings of the left side door column joints vs. the horizontal top displacements (LVDT 32).

In fact, damage is concentrated on the joint immediately above the near the basement joints, i.e. spots 5 and 13. This situation is confirmed by the formation of an inclined strut from the top up to that spot, confirmed by an extensive crack towards this direction (Fig. 7). One can, therefore, conclude that the door column base is a more rigid area, meaning a lower damage concentration. This might be explained by the concrete foundation, which brought a further rigidity to this area.

Fig. 7. Wall after the experiment.

2.4 *LVDT 5 and 13*

These joints showed a quite unusual behavior, since their performance is alike. Instead of showing an alternate behavior like the previous ones, the joints opened and closed at the same time. This might have happened due to the configuration of the stones and to the cut surfaces that appeared during the test. These cut surfaces result from the fact that this is a short column type structure, quite heterogeneous, with low cohesion between its constituent elements (blocks and infill) and no tensile strength. In fact, when activated by the horizontal forces, the wall follows a Strut and Tie type behavior model. According to this model, the wall resists the applied horizontal forces through its most rigid elements along a diagonal strut. However, since the wall showed a stronger resistance at the basement, damage was then concentrated immediately above the door column joints (5, 13). The damage concentration on this area could be observed through a simple analysis of the results concerning the displacements at the door column intermediate joints (Fig. 8 and 9). In particular, the horizontal displacements of the door columns in Figure 9 (23, 30, 31, 32) for the maximum applied top displacement (10mm) in the negative direction show a larger displacement in both central LVDTs than in the higher LVDTs

(which, theoretically, should show the higher displacements). This larger displacement at the central area represents a larger damage concentration at the intermediate areas.

Finally, the compression forces draw cracks along the wall, which tend to follow the stones' joints. These cracks delimit the above referred sliding/cut surfaces.

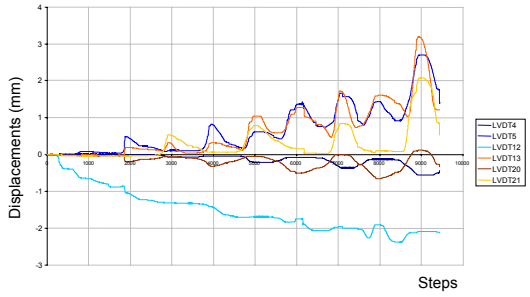

Fig. 8. Joints opening at the door columns.

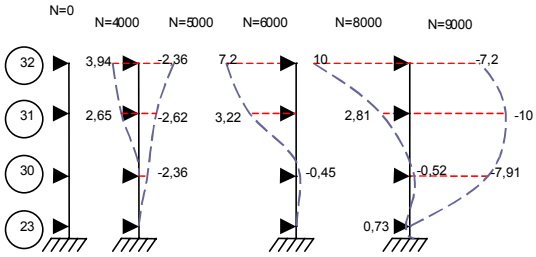

Fig. 9. Scheme representing the door columns movement during the test.

2.5 *LVDT 12 and 21*

The LVDT 12 data was unusual. The behavior of this joint was opposite to what was expected. As the cyclical horizontal displacements were imposed, instead of opening (for displacements in the positive direction) and closing (for displacements in the negative direction), the joint displacement trend was always towards closure (almost 2.5mm), and in no occasion was there a displacement towards compression decrease and joint opening. The reason for this behavior lies in the fact that the wall before the test was accidentally damaged at the spot where the LVDT 12 was positioned (Fig. 10). Although the stones were reset into their original position, this measure was inefficient to reproduce the expected behavior of the wall on that area; the existing link between the materials, as well as the right contact between the stones was lost. On the contrary, the joint at spot 21 acted as predicted, with a closing trend upon horizontal displacements applied in the positive direction and an opening trend upon horizontal displacements applied in the negative direction. This joint showed an opening of ~2.0mm.

As aforementioned, the damage inflicted to the high, right corner of the wall (12) before the test distorted the outcome and made impracticable a comparison between these two LVDTs results.

Fig. 10. Damaged area.

2.6 *Analysis of the Force - Displacement graphic*

As the force versus displacement curve in Figure 11 shows, the masonry wall posses a good energy dissipation capacity and, interestingly, has a performance similar to the one of a reinforced concrete element. Notice that for displacements imposed in the positive direction, the wall loses resistance in successive loading cycles for the same displacement figure. In particular, from the 4mm loading cycle to the 6mm loading cycle, there was a local resistance loss at 4mm of ~ 20%, which was recovered at the cycle end, i.e. for the 6mm displacement. Furthermore, the last loading cycle shows that a nonrecoverable lost of strength might have occurred, since the curve seems incapable of recovering the previous cycle strength capacity.

Simultaneously, the curve for the displacements on the other direction shows lower dissipation of energy. In fact, the wall was not similarly loaded in both directions. However, if a symmetrical load had been performed, a similar dissipated energy would be expected in both directions, as well as a similar strength lost at each displacement cycle in both directions.

The structure rigidity also decreased during cyclic loading.

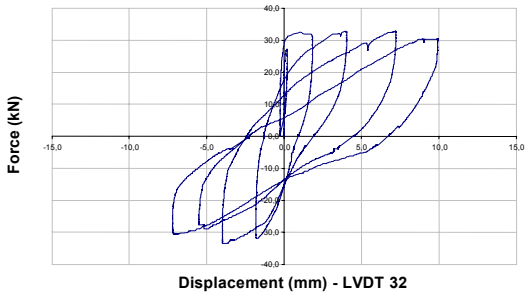

Fig. 11. Horizontal top force vs. top displacement curve.

2.7 *Analysis of the wall vertical rotation*

Considering the proposed goals for this test, the ideal situation would be that no vertical rotation of the wall should occur; in other words, the horizontal displacements should be applied on the wall rigidity center. However, as Figure 12 shows, the wall top section rotates. At the beginning and as the horizontal displacement occurs, the wall rotates into a certain direction; from step 2500, the wall rigidity center must have changed its position as a result of an inside rearrangement of the stone blocks, and the wall top section rotates in the opposite direction.

The LVDTs 28 and 29 also show that the wall moves in the transverse direction.

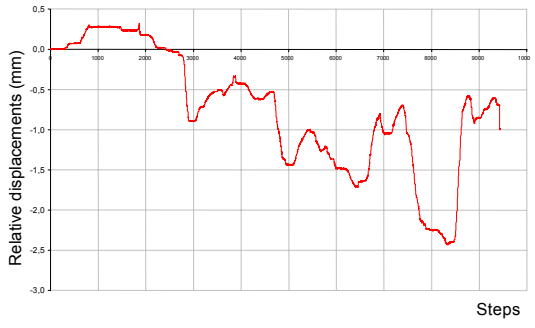

Fig. 12. Relative transverse displacement of the wall top section: (LVDT 28) – (LVDT 29).

3 METHODOLOGY FOLLOWED TO BUILD A NUMERICAL MODEL

3.1 *Methodology*

The wall was then simulated using a finite-element method. To define the geometry underlying the numerical modeling it was necessary to make a geometric survey of the wall. The wall external outline was measured and the wall mortar was removed to get a clear view of the main stones geometry. This wall observation and survey was followed by the definition of the finite-elements mesh. This procedure involved the use in sequence of several auxiliary programs (AutoCad 2004, Solidworks 2004, GiD 7.5.0b, and a program called BLOCO). All these programs were necessary to convert the Autocad and Solidworks defined geometries into the language Gibiane of CAST3M finite-element program. Basically, CAST3M is a computer code for analyzing structures using finite-elements methodologies that was developed by the French Commission for Atomic Energy (CEA). The CAST3M is high-level tool for civil engineering investigation purposes and it integrates pre- and post-processing functions.

In the first stage, the wall base geometry was defined with the help of Autocad 2004 and was saved in a DXF format file. However, the information organized in DXF format is not easily transferable to the CAST3M input file, which is based on a unique language called Gibiane (a set of commands, operators and objects are internally interpreted by the CAST3M base code). To do so, two programs, SolidWorks 2004 and GiD, were used. The SolidWorks 2004 enabled the interpretation of the blocks geometry from the Autocad information and the definition of each block as a volume (3D solid) that later was saved in PARASOLID format. These files containing each block were later introduced in the same SolidWorks object, so that the whole wall geometry could be observed. From this initial geometry, it was necessary to carry out an interactive process, in order to get the most accurate approach to the wall geometric form, as illustrated on Figure 13. The GiD is a pre- and post-processing program for numerical analysis based on the finite-elements method. The use of this program allowed the interpretation of DXF files from Autocad 2004 and to keep in a file only the information needed to define the wall geometry. Finally, the auxiliary program BLOCO was used to recover the information resulting from

GiD and to transfer it into Gibiane format, capable of being interpreted by CAST3M.

In an initial stage, the stiff structure at the top of the wall was not simulated, in order to calibrate the material properties: the elastic modulus, the Poisson coefficient, and the volume weight, by achieving the natural frequencies and comparing them to those obtained in the physical model in identical conditions. These parameters were refined starting from values obtained from tests performed in the past to walls with similar characteristics (with stone blocks and infill). In the link between elements (block to block or block to infill), joints with a Coulomb nonlinear friction model without dilation were used. The model is defined through three constants, tnt, kn, ks, and two material behavior laws (one for transverse and the other for normal stresses and displacements).

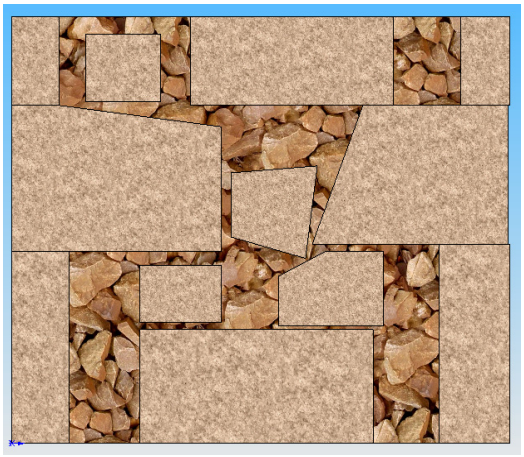

Fig. 13. The 3D image of the wall in SolidWorks and the actual picture of the wall.

After calibrating the model parameters, the stiff structure at the top of the wall was introduced. Regarding the nonlinear model to be used for the infill and the joints, it was decided to use a reinforced concrete type model for the infill (since no soil type model existed in CAST3M with the requested characteristics) and a trilinear shear/sliding law for the joints. The nonlinear analysis was performed first for a monotonic load until a maximum 10mm horizontal displacement was reached at the top, and afterwards, for a cyclic law similar to the displacement law obtained during the test.

3.2 *Numerical results*

The numerical horizontal top force versus top displacement results are represented in Figure 14. Figure 15 shows the stresses chart for the maximum displacement of the monotonic law. Figures 16 and 17 represent the deformed shapes for maximum displacements in both directions for the cyclical loading. These are the most relevant results for interpretation and later comparison with those observed at the experimental test.

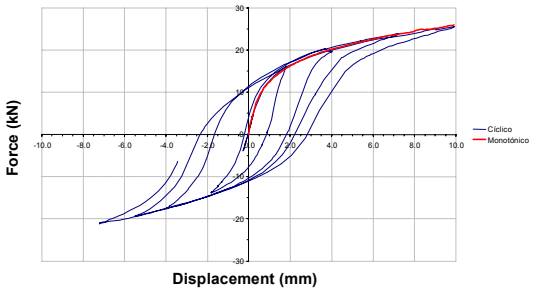

Fig. 14. Numerical horizontal top force vs. top displacement curve for the monotonic and cyclic load.

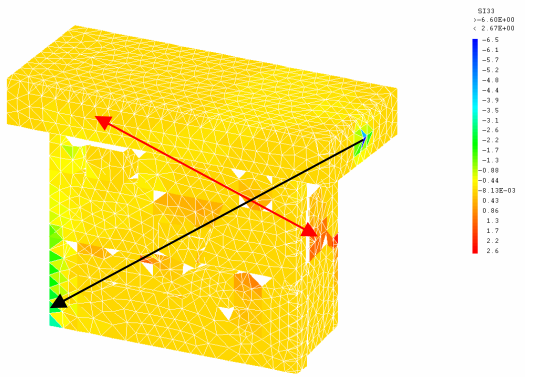

Fig. 15. Chart of the main compression stresses σ_{33} at the wall.

3.3 *Analysis of the results*

The analysis of Figure 14 shows that the selected model provides good energy dissipation and a maximum resisting force of around 26kN. On the other hand, from Figure 15, one can assume that the load is transmitted from the top to the foundation through a strut and a tie.

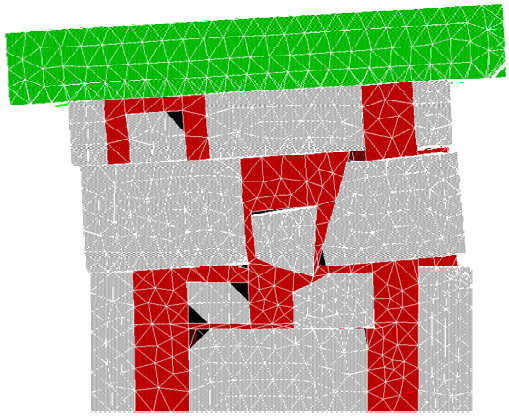

Fig. 16. Deformed shape at the +10mm displacement during cyclic loading.

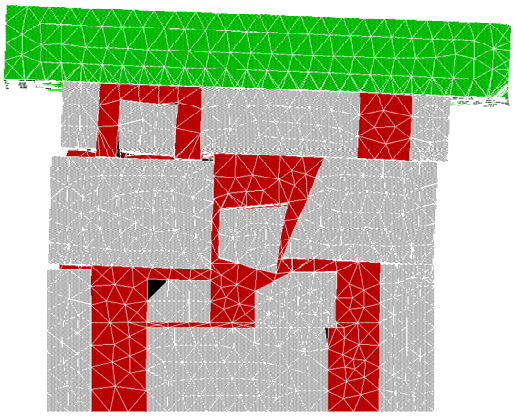

Fig. 17. Deformed shape at the -7.2mm displacement during cyclic loading.

Reviewing Figures 16 and 17, the wall shows a behavior with sliding at two levels, following the almost continuous horizontal joints surfaces quite evident in the two figures. Moreover, most of the displacements occur at these two sliding levels. For positive displacements (Fig. 16) the transverse bending of the wall is almost zero. However, there is a slight vertical rotation of the wall, meaning that the rigidity center is not located on the line of the applied force.

As for negative displacements (Fig. 17), the wall bends in the transverse direction, weakening the links between the different front elements.

3.4 *Comparison with the experimental results*

By comparing the experimental results with those of the numerical model, one is forced to conclude that the model used to characterize the infill was inappropriate, showing lower rigidity than the one observed at the physical model (Fig. 18). Besides, some properties typical of such kind of walls, such as the link between the materials, could not be reproduced in the numerical model. However, values such as the peak force or the horizontal displacement at two thirds of the wall height (Fig. 19) are quite close to those achieved during the experimental test. These values show that more accurate results could have been obtained if another type of model had been used to characterize the infill. On the other hand, the numerical model managed to reproduce the rotations and the horizontal displacements of the wall during the test. Besides the energy dissipation and the forces transmission mechanisms, the sliding surfaces and the blocks movements were sufficiently well reproduced and located through this model too.

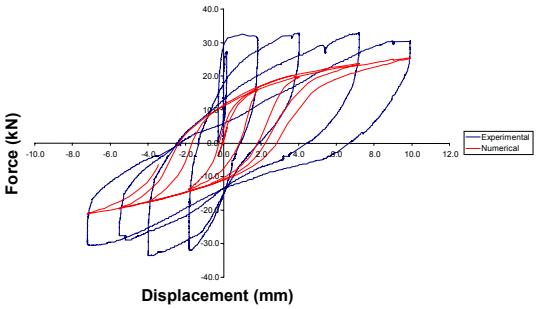

Fig. 18. Numerical and experimental horizontal top force vs. top displacement curves.

4 WALL REINFORCEMENT

4.1 *Presentation of the adopted reinforcement solution*

After the experimental test, the wall was reinforced using a process that is commonly used in the Archipelago of Azores. The process consists first of introducing steel rods (4 in this case) in the transverse direction of the wall in order to link both sides of the structure. Then, the joints between the

blocks are filled up with mortar. Afterwards, a metallic net is set around the whole wall and metallic plates (60 × 40cm^2) are set on the ties and tightened against the wall (Fig. 20), so that the steel rods and the metallic net act together with the wall, reinforcing it. Another metallic net is set on the metallic plates to enable bonding with the mortar. Then the metal structure is fixed to the wall on the sides through screws, and the ties are cut to prepare the wall to receive mortar (Fig. 21). Finally, the wall was covered with plastic to simulate the Azores concrete cure conditions, with a high air moisture percentage (Fig. 22).

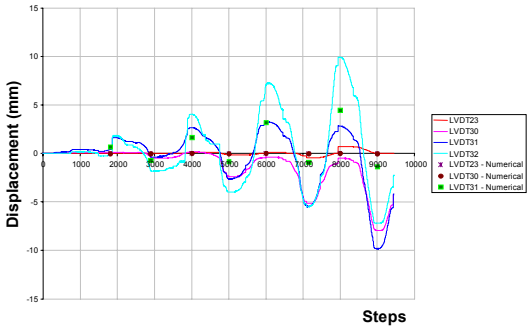

Fig. 19. Horizontal displacements obtained both with the numerical and the experimental models.

4.2 *Test methodology and results analysis*

The methodology and apparatus adopted for testing the reinforced wall were the same adopted for testing the nonreinforced wall. The same loading history was considered plus another two 10mm cycles, and three 14mm and 17.5mm cycles.

The results were quite different from those of the nonreinforced wall. The most relevant are presented. Figure 23 shows the horizontal top force versus top displacement curve, and Figure 24 the joints opening evolution. Unlike the behavior of the nonreinforced wall, the reinforced wall acted as a block; there was no sliding between successive levels. The wall acted as a block, with only a joint opening on the base, as can be observed in Figures 24 and 25. In Figure 23, one observes that for the same displacement level the reinforced wall showed greater resistance than the nonreinforced wall. The maximum resistance of the reinforced wall is ~100kN, almost three times higher than the nonreinforced wall (~35kN).

High and intermediate joints in both door columns show an almost null displacement. The joints at the basement (4, 20) showed a consistent behavior: when one of the joints opened, the other closed and vice-versa. Both developed extensive opening displacements, which became quite visible during the test. In fact, all damage was concentrated on the bottom of the wall. This behavior was quite distinct from that obtained for the nonreinforced wall. Here there was joint movement and a more spread damage with extensive cracking of the wall facades.

Fig. 20. Reinforcing technique: metallic net and steel rods.

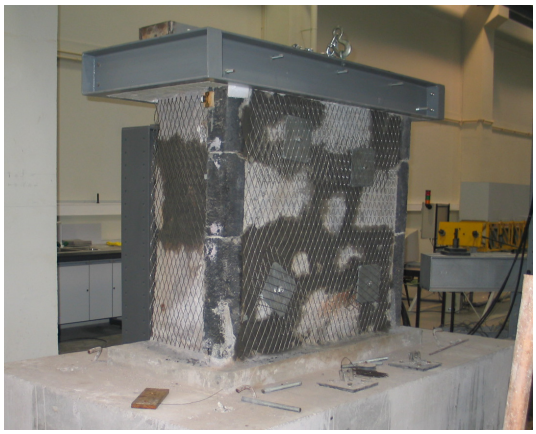

Fig. 21. Wall view before covering with mortar.

Fig. 22. Simulation of local air moisture conditions.

Finally, Figure 23 shows that a lower dissipation of energy should be expected when the wall is reinforced with this technique.

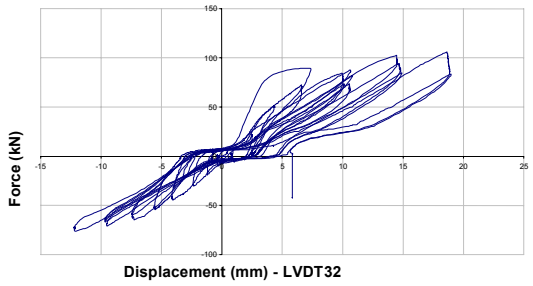

Fig. 23. Horizontal top force vs. top displacement curve for the reinforced wall.

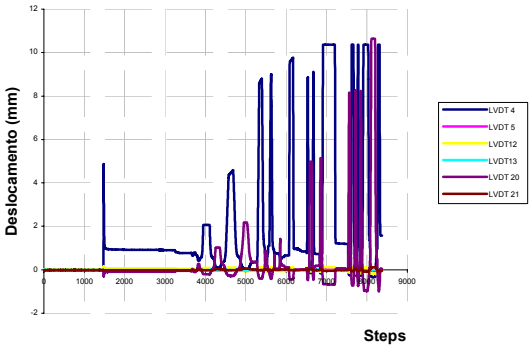

Fig. 24. Evolution of the joints opening for the reinforced wall.

5 CONCLUSIONS

The reinforced wall showed in general a better behavior than the nonreinforced wall. This means that the current reinforcement process used today in the Archipelago of Azores is most effective against horizontal actions. Besides the safety factor, it should be stressed that the performance of the reinforced wall, regarding cracking and higher displacement levels than those responsible for cracks in the nonreinforced wall, did not show any cracking in the entire wall, but only at the basement. This behavior proves the reinforcement efficiency, since it stopped the wall from acting as a heterogeneous, easily deforming conglomerate made up of "glued" stones by a low cohesion infill, and made it act as a single rigid entity. However, lower dissipation of energy should be expected.

As for the numerical simulation, it can be concluded that the outcome of the numerical model is reasonable, considering the complexity of the adopted model. However, further work should be carried out to better simulate the infill behavior, by exploring other type of models or even by creating a new model type. Furthermore, new solutions should be pursued to introduce other phenomena in the models, which were not considered in this work but have a strong influence in the wall's final behavior; for instance, the link between normal stress force in the horizontally or vertically positioned joints between blocks and fill material.

6 ACKNOWLEDGEMENTS

The authors would like to express their regards to all people and entities that in any way contributed to this paper; namely, Cristina Costa for her constant support and all employees of the LESE, mainly Daniela for her interest and support.

7 REFERENCES

Almeida, C. 2000. Análise do Comportamento da Igreja do Mosteiro da Serra do Pilar sob a Acção dos Sismos. Tese de Mestrado em Engenharia Civil, Faculdade de Engenharia da Universidade do Porto, Porto, Portugal.

CEA 1990 – CASTEM 2000. Guide d'utilisation, CEA, Saclay, França.

Costa, C. 2002. Análise do Comportamento da Ponte da Lagoncinha sob a Acção do Tráfego Rodoviário. Tese de Mestrado em Engenharia Civil, Faculdade de Engenharia da Universidade do Porto, Porto, Portugal

Costa, A. G. 1999. Ensaios de Caracterização de Alvenarias Tradicionais. Secretaria Regional de Habitação e Equipamentos, Açores, Portugal.

Daniela, 2004. Relatório das características técnicas das Células de Carga 09,10,11,12. LESE, Porto, Portugal.

Faria, R. 1994. Avaliação do Comportamento sísmico de Barragens de Betão através de um Modelo de Dano Contínuo. Tese de Douturamento em Engenharia Civil, Faculdade de Engenharia da Universidade do Porto, Porto, Portugal.

Pegon, P. 1999. Automatic Generation of Blocks Connected with Joints in CASTEM 2000. Special Publication No. I.99.101, ISIS, SMU, JRC, Ispra (VA), Italia.

Pegon, P. & Pinto, A.V. 1996. Seismic Study of Monumental Structures – Structural Analysis, Modelling and Definition of Experimental Model. Report EUR 16387 EN, ISIS, SMU, JRC, Ispra (VA), Italia.